Journal of
NANOSTRUCTURES
JNS
NANOSTRUCTURES
JNS.kashanu.ac.ir

Sol-gel Synthesis of ZnO Nanoparticles and ZnO-TiO_2-SiO_2 Nanocomposites and Their Photo-catalyst Investigation in Methylene Blue Degradation

B. Kaleji [a]*, M. Mousaei[a], H. Halakouie [b], A. Ahmadi [b]

[a] *Department of Materials Engineering, Malayer University, Malayer, Iran*

[b] *Department of Physics, Faculty of Science, Arak University, Arak 38156-88349, Iran*

Received 15/07/2015
Accepted 20/08/2015
Published online 01/09/2015

Keywords:
Sol-gel
ZnO-TiO_2-SiO_2
Nanocomposites

**Corresponding author:*
E-mail address:
b.kaleji@malayeru.ac.ir
Phone: +98 912 4389249
Fax: +98 86 34173406

Abstract

In this work firstly ZnO nanoparticles were synthesized via a simple precipitation method. At the second step titanium dioxide and silicon dioxide shell were synthesized on the core. For preparation ZnO-TiO_2-SiO_2 the sol product was calcinated at 500 ºC for 2h. Properties of the product were examined by X-ray diffraction pattern (XRD), scanning electron microscope (SEM) and Fourier transform infrared (FT-IR) spectroscopy. The photo-catalytic behavior of ZnO-SiO_2-TiO_2 nanocomposite was evaluated using the degradation of a methylene blue aqueous solution under visible light irradiation. The results show that ZnO-SiO_2-TiO_2 nanocomposites have applicable photo-catalytic performance.

1. Introduction

Different methods to eliminate pollutants compounds from wastewater have been reported in the literature; among them, the advanced oxidation processes, in which the photo-degradation processes are included. These processes consist in the decomposition of organic molecules interacting with both, an UV or visible light as well as the interaction with a photo-catalyst material, in order to get CO_2 and H_2O as final products [1-3]. For its low toxicity, good biocompatibility and tunable properties, ZnO have received considerable attention in various areas such as catalysis, systems, drug delivery and turgeting, anti bacterial, cancer therapy and enzyme immobilization [5-6].

Several semiconductor materials have been reported in the literatureas such as TiO_2 (effective and most frequently mentioned) ZrO_2, WO_3, ZnO, ZnS, SnO_2, Fe_2O_3, as well as large number of binary, ternary and quaternary mixed oxides[1, 6-9].

There is an increasing interest in nanoparticles because of their broad applications in several technological fields

including drug delivery, microwave devices, and high density information storage [10-13]. ZnO has been widely studied because it possesses excellent chemical stability and suitable anti bacterial. In addition to the precise control on the composition and structure of ZnO different chemical and physical synthesis methods, such as precipitation, sol-gel, hydrothermal are used to produce magnetite. Among the reported methods, the sol-gel method is an efficient way to production of ultrafine and mono-dispersed powder [14-20].

A variety of synthesis strategies for metal hydroxides nanostructure materials have been described. Sol-gel method as a simple, effective and novel route has been developed to prepare nanostructures.

Photo-catalysts have gained much attention because those can easily be seperated from polluted waters by applying a simple magnetic field.

In the present work, ZnO nanoparticles and ZnO-TiO_2-SiO_2 nanocomposites were synthesized by a simple sol-gel method without using inert atmosphere. The obtained samples were characterized by scanning electron microscopy and X-ray diffraction pattern.

2. Experimental

2.1. Materials and Instruments

Zinc acetate, ethyl aceto acetate, ethyl aceto acetate, tetraethyl orthosilicate, mono ethanol amine and titanium tetra iso propoxide were purchased from Merck Company. All of the chemicals were used as received without further purifications. XRD patterns were recorded by a Philips, X-ray diffracttometer using Ni-filtered Cu K_α radiation. For SEM images the samples were coated by a very thin layer of Au to make the sample surface conductor and prevent charge accumulation, and obtaining a better contrast.

A multiwave ultrasonic generator (Sonicator 3000; Bandeline, MS 73, Germany), equipped with a converter/transducer and titanium oscillator (horn), 1.25×10^{-2} m in diameter, surface area of ultrasound irradiating face: 1.23×10^{-4} m^2, operating at 20 kHz, was used for the ultrasonic irradiation and the horn was operated at 50% amplitude. All ultra-sonication experiments were carried out at ultrasonic power between 84–125 mW measured by calorimeter.

2.2. Synthesis of ZnO nanoparticles

2.2 g of zinc acetate was dissolved in mixture of 20 ml of ethanol and 1.2 ml of mono ethanol amine. 1.8 ml of water is slowly added to the solution. A white precipitate is obtained confirming the synthesis of ZnO. The precipitate of ZnO is then centrifuged and rinsed with distilled water, followed by being left in an atmosphere environment to dry.

2.3. Synthesis of nanocomposites

20 ml of ethanol and 2.5 ml of ethyl aceto acetate were mixed together.3ml of titanium tetra iso propoxide was added to solution. 0.6 ml of HNO_3 and 1.8 ml of water was added to the solution. Sol of SiO_2 was prepared as follow:

20 ml of ethyl aceto acetate and 2.4 ml of tetraethyl orthosilicate were mixed together. 0.6 ml of HNO_3 and 1.8 ml of water was added to the solution.

For preparation of different nanocomposites various amounts of three components were mixed

and were calcinated at 500 ºC (400 or 600 ºC) for 2h.

3. Results and discussion

The XRD pattern of ZnO nanoparticles is shown in Fig. 1. The pattern of as-prepared ZnO nanoparticles is indexed as a pure cubic phase which is very close to the literature values (JCPDS No. 79-0208). Space group of magnetite is Fd3m. The narrow sharp peaks indicate that the ZnO nanoparticles are well crystallized.

The crystallite size measurements were also carried out using the Scherrer equation,

$$D_c=K\lambda/\beta Cos\theta$$

Where β is the width of the observed diffraction peak at its half maximum intensity (FWHM), K is the shape factor, which takes a value of about 0.9, and λ is the X-ray wavelength (CuK_α radiation, equals to 0.154 nm). The estimated crystallite size was about 14 nm.

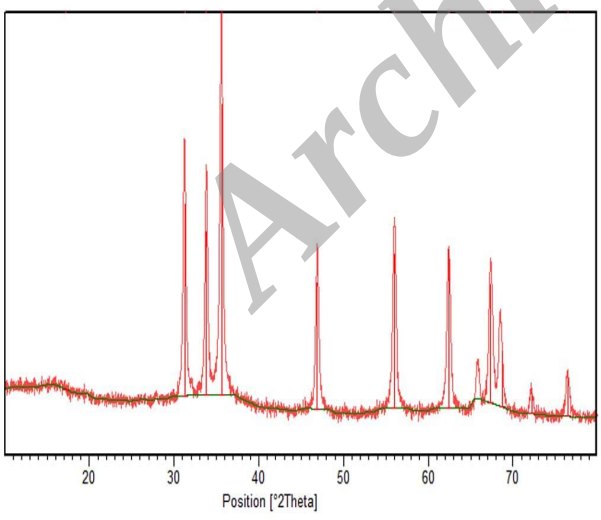

Fig. 1. XRD pattern of the ZnO nanoparticles

The XRD pattern of ZnO-SiO_2-TiO_2 (90/5/5) nanoparticles is illustrated in Fig. 2. The pattern of ZnO nanoparticles show a pure hexagonal phase which is very close to the literature values (JCPDS No. 79-0208).

The XRD pattern of ZnO-SiO_2-TiO_2 (80/10/10) nanocomposite is shown in Fig. 3. The pattern of nanocomposite shows three phases of zinc oxide, TiO_2 and SiO_2. SiO_2 has a broad peak around 2theta:2-30 that is shown in Fig. 2 and Fig. 3.

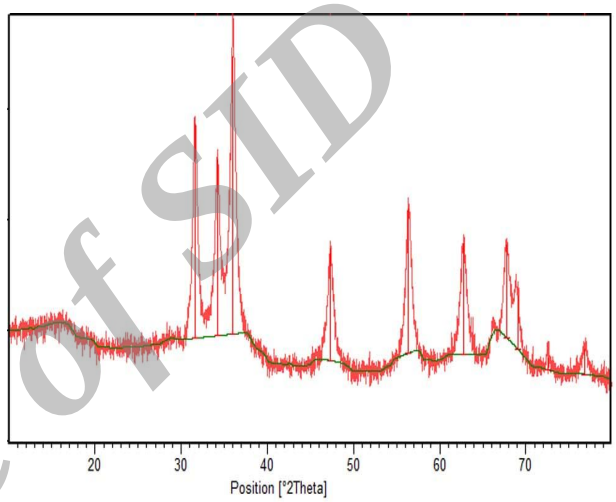

Fig. 2. XRD pattern of the ZnO-SiO_2-TiO_2 (90/5/5) nanocomposite

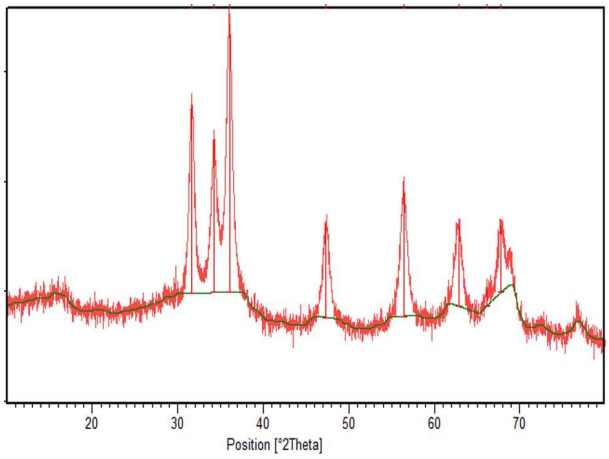

Fig. 3. XRD pattern of the ZnO-SiO_2-TiO_2 (80/10/10) nanocomposite

Fig. 4 illustrates scanning electron microscopy images of synthesized ZnO nanoparticles that

confirm average diameter size of product is less than 90 nm.

SEM images of ZnO-SiO_2-TiO_2 at ratio of 90/5/5 are studied and are illustrated in Fig.5. According to images particles with average diameter of 100 nm are obtained.

The image shows that the sample consists of larger particles compare to pure zinc oxide nanoparticles.

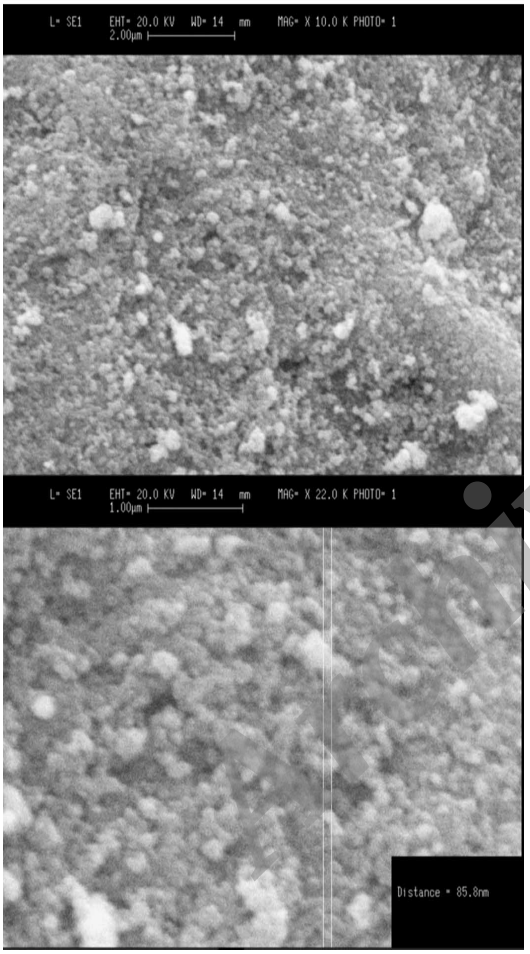

Fig. 4. SEM images of ZnO nanoparticles

Fig. 6 illustrates SEM images of ZnO-SiO_2-TiO_2 nanocomposite that is obtained at ratio of 80/10/10 and confirms some agglomeration compare to 90/5/5. It seems growth stage is predominant compare to nucleation stage.

Fig. 7 shows SEM images of ZnO-SiO_2-TiO_2 nanocomposite that is obtained at 500 ºC and 85/10/5 and confirms some agglomeration compare to pure ZnO nanoparticles. It approves molar ratio appropriately effect on the particle size and morphology of the product.

The effect of temperature on the morphology of the product was investigated at lower temperature at 400 ºC bigger products were obtained (Fig. 8a) and also at 600 ºC particles with average particle size of 90 nm were achieved that are higher than product synthesized at 500ºC (Fig. 8b).

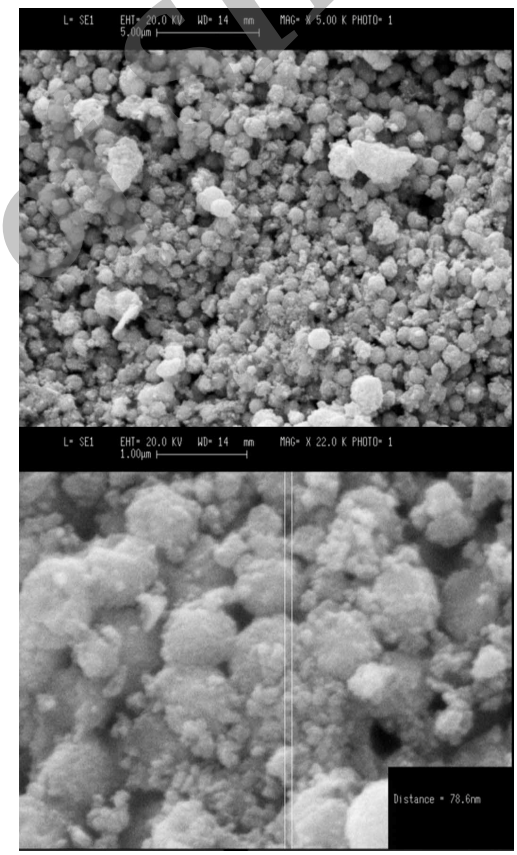

Fig. 5. SEM images the ZnO-SiO_2-TiO_2 (90/5/5) nanoparticles

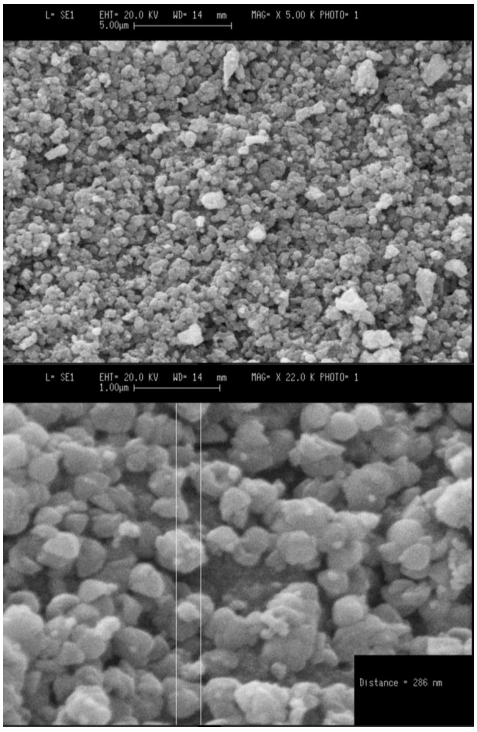

Fig. 6. SEM images of ZnO-SiO_2-TiO_2 (80/10/10) nanocomposite

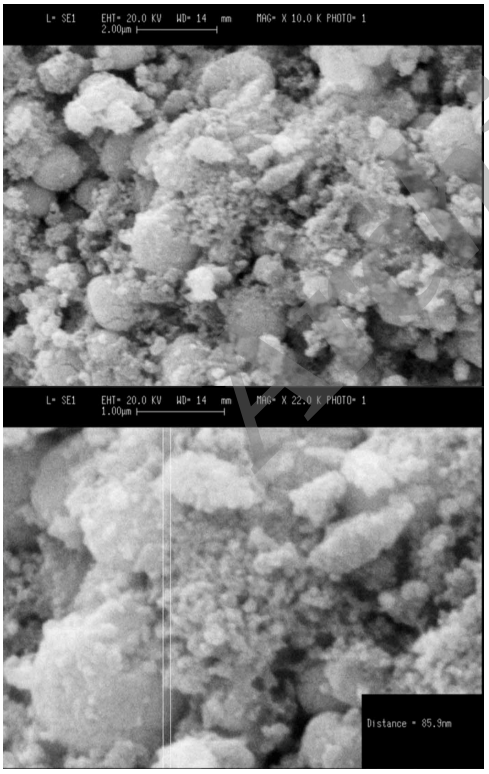

Fig. 7. SEM images of ZnO-SiO_2-TiO_2 (85/10/5) nanocomposite

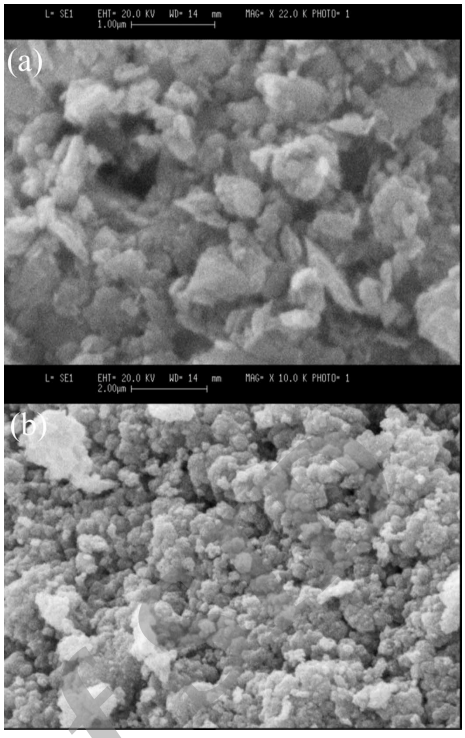

Fig. 8. SEM image of ZnO-SiO_2-TiO_2 (a) 400 ^oC (b) 600 ^oC nanocomposite

Fourier transform infra-red (FT-IR) spectrum of synthesized nanoparticles was recorded in the range of 400–4000 cm^{-1} and result is shown in Fig. 9. Absorption peaks around 400 to 500 cm^{-1} are related to metal-oxygen Zn-O bonds. The spectrum exhibits broad absorption peaks between 3500-3600 cm^{-1}, corresponding to the stretching mode of O-H group of hydroxyl group that are adsorbed on the surface of nanoparticles.

FT-IR spectrum of prepared ZnO-SiO_2-TiO_2 nanoparticles in the range of 400–4000 cm^{-1} is shown in Fig. 10. Absorption peaks around 437 is related to Zn-O bonds. The spectrum exhibits broad absorption peaks between 3500-3600 cm^{-1}, corresponding to the stretching mode of O-H group of hydroxyl group that are adsorbed on the surface of nanoparticles. Peak at 941 cm^{-1} is responsible to Si-O bonds.

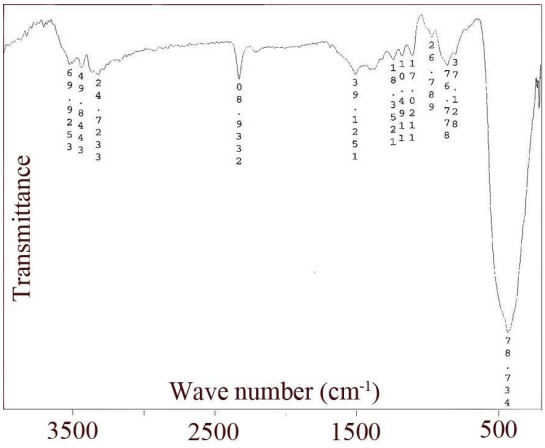

Fig. 9. FT-IR spectrum of ZnO nanoparticle

The photo-catalytic activity of the nanocomposite was evaluated by monitoring the degradation of methylene blue (MB) in an aqueous solution. 0.1 g of nanocomposite was dispersed in 10 ml of MB solution (5ppm). Pure methylene blue and MB under UV visible in the presence of ZnO-SiO_2-TiO_2 (60 and 120 min) are illustrated in Fig 11a-c respectively.

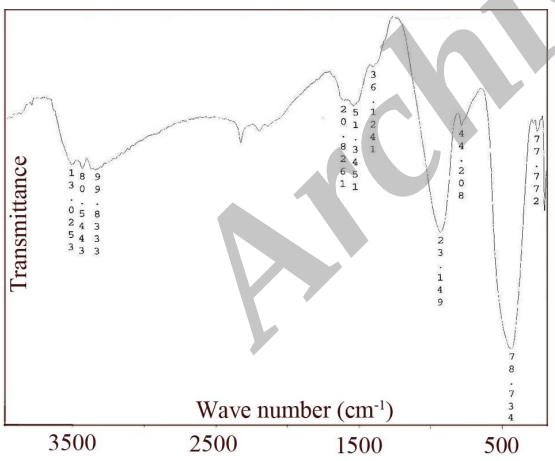

Fig. 10. FT-IR spectrum of ZnO-SiO_2-TiO_2 nanocomposite

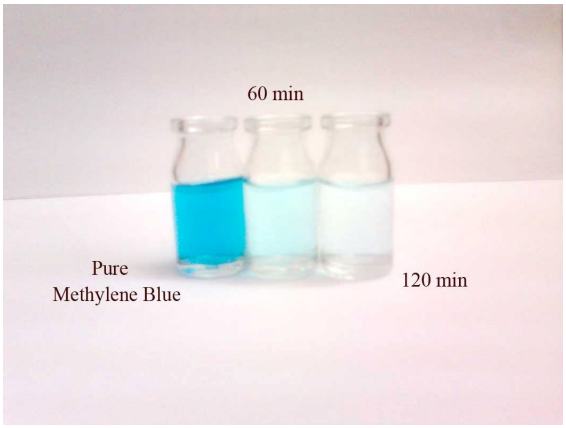

Fig. 11. Effect of ZnO-SiO_2-TiO_2 (a) Methylene blue (b) 60 min (c) 120 min

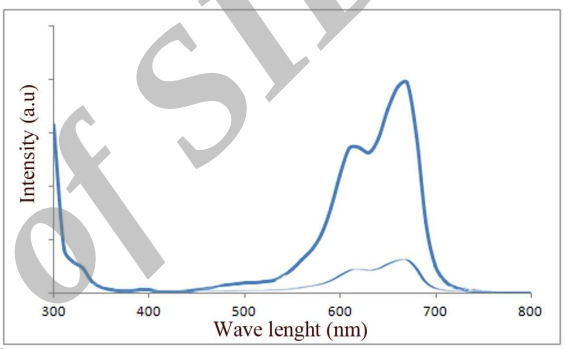

Fig. 12. Effect of ZnO-SiO_2-TiO_2 under UV irradiation (a) Methylene blue (b) 120 min

As time increased, more and more MB were adsorbed on the nanocomposite catalyst, until the absorption peak vanish. The MB concentration decreased rapidly with increasing time, and the peak almost disappeared after 120 min. UV-visible spectra of pure methyl blue and methyl blue in presence of nanoparticles are shown in Fig 12a and b respectively.

4. Conclusion

Photocatalyst ZnO nanoparticles were synthesized via a precipitation method. Then SiO_2 and TiO_2 shell was synthesized on the ZnO core. For synthesis ZnO- TiO_2-SiO_2 the product was calcinated at 500 ºC for 2h. The photocatalytic

behavior of $ZnO-TiO_2-SiO_2$ nanocomposite was evaluated using the degradation of a methyl blue aqueous solution under visible light irradiation. The results show that $ZnO-TiO_2-SiO_2$ nanocomposites are promising materials with suitable performance in photo-catalytic applications.

References

[1] S. Moshtaghi, M. Salavati-Niasari, D. Ghanbari, J Nano Struc 5 (2015) 169-174

[2] F. Tzompantzi, Y. Pina, A. Mantilla, O. Aguilar-Martínez, F. Galindo-Hernandez, Xim Bokhimi, A. Barrera. Catal Today 222 (2014) 49–55.

[3] H.R. Momenian, M. Salavati-Niasari, D. Ghanbari, B. Pedram, F. Mozaffar, S. Gholamrezaei, J Nano Struc. 4 (2014) 99-104.

[4] F. Zhang, S. Kantake, Y. Kitamoto, M. Abe, IEEE Trans. Magn. 35 (1999) 2751–2753.

[5] Y. Kitamoto, S. Kantake, S. Shirasaki, F. Abe, M. Naoe, J. Appl. Phys. 85 (1999) 4708-4710.

[6] A.E. Berkowitz, W. Schuele, J. Appl. Phys. 30 (1959) 134–135.

[7] D. Ghanbari, M. Salavati-Niasari, M. Ghasemi-Koch, J Indus Eng Chem. 20 (2014) 3970-3974.

[8] G. Nabiyouni, S. Sharifi, D. Ghanbari, M. Salavati-Niasari, J Nano Struc. 4 (2014) 317-323.

[9] X. Chu, D. Jiang, Y. Guo, C. Zheng, Sens. Actuator B. 120 (2006) 177.-181

[10] C.C. Wang, I.H. Chen, C.R. Lin, J. Magn. Magn. Mater. 304 (2006) 451-453.

[11] Y.I. Kim, D. Kim, C.S. Lee, Phys. B 337 (2003) 42-51.

[12] Y. Shi, J. Ding, H. Yin, J. Alloys Compd. 308 (2000) 290-295.

[13] S. Gholamrezaei, M. Salavati-Niasari, D. Ghanbari, J Indus Eng Chem. 20 (2014) 3335-3341.

[14] K. Maaz, A. Mumtaz, S.K. Hasanain, A. Ceylan, J. Magn. Magn. Mater 308 (2007) 289-295.

[15] S. Gholamrezaei, M. Salavati-Niasari, D. Ghanbari, J Indus Eng Chem. 20 (2014) 4000-4007.

[16] H.R. Momenian, S. Gholamrezaei, M. Salavati-Niasari, B. Pedram , F. Mozaffar , D. Ghanbari, J Clust Sci. 24 (2013) 1031-1042.

[17] D. Ghanbari, M. Salavati-Niasari, S. Karimzadeh, S. Gholamrezaei, J NanoStructures 4, (2014) 227-232.

[18] L. Nejati Moghadam; A. Esmaeili-Bafghi, M. Salavati-Niasari, H. Safardoust, J NanoStructures 5, (2015) 47-53

[19] M. Panahi-Kalamuei, M. Mousavi-Kamazani, M. Salavati-Niasari, J NanoStructures 4, (2014) 459-465.

[20] F. Beshkar; M. Salavati-Niasari, J NanoStructures 5, (2015) 17-23